

Is it an i or an l: Test-time Adaptation of Text Line Recognition Models

Debapriya Tula, Sujoy Paul, Gagan Madan, Peter Garst, Reeve Ingle, Gaurav Aggarwal

Google Research

Abstract

Recognizing text lines from images is a challenging problem, especially for handwritten documents due to large variations in writing styles. While text line recognition models are generally trained on large corpora of real and synthetic data, such models can still make frequent mistakes if the handwriting is inscrutable or the image acquisition process adds corruptions, such as noise, blur, compression, etc. Writing style is generally quite consistent for an individual, which can be leveraged to correct mistakes made by such models. Motivated by this, we introduce the problem of adapting text line recognition models during test time. We focus on a challenging and realistic setting where, given only a single test image consisting of multiple text lines, the task is to adapt the model such that it performs better on the image, without any labels. We propose an iterative self-training approach that uses feedback from the language model to update the optical model, with confident self-labels in each iteration. The confidence measure is based on an augmentation mechanism that evaluates the divergence of the model's prediction in a local region. We perform rigorous evaluation of our method on several benchmark datasets as well as their corrupted versions. Experimental results on multiple datasets spanning multiple scripts show that the proposed adaptation method offers an absolute improvement of up to 8% in character error rate with just a few iterations of self-training at test time.

1 Introduction

Text line recognition (Diaz et al. 2021; Li et al. 2021) has been a challenging problem in the field of computer vision and machine learning for several decades. The task of recognizing handwritten text involves understanding and interpreting human handwriting - having a free flowing nature (Bhunia et al. 2019) - in various languages and styles, making it a complex and multifaceted problem. Over the years, various sophisticated models (Diaz et al. 2021; Ingle et al. 2019; Li et al. 2021; Breuel et al. 2013; Long, He, and Yao 2021) have been developed, which are trained on large corpora of labeled and synthetic data. However, recognizing handwriting data still remains a challenge due to large variations in styles across individuals. Additionally, the image acquisition process often adds corruptions such as blur, noise, compression, making recognition even more challenging. Deep learning models are often known to have generalization issues leading to significant drop in performance for

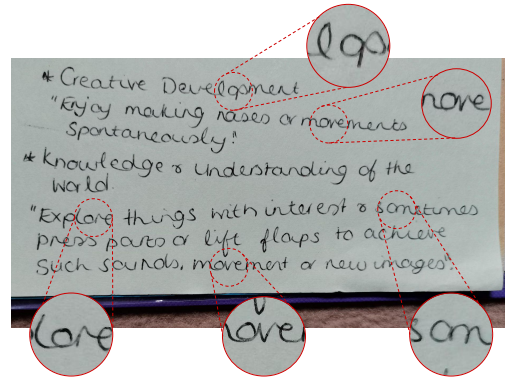


Figure 1: Sample image from the GNHK dataset (Lee, Chung, and Lee 2021) showing how the letter "o" might look like "q" or "a" in handwritten text, which is the writer's style. We want our algorithm to adapt to such styles on the fly during test time.

distribution shifts (Hoffman et al. 2018; Tsai et al. 2018), corruptions (Hendrycks and Dietterich 2019), etc. This is no different for text line recognition. To solve this problem, we develop an algorithm to adapt an existing text line recognition model to specific writing styles during test time, given only a single test image.

Unsupervised domain adaptation (Hoffman et al. 2018; Tsai et al. 2018) is a well-studied problem, where the task is to adapt a model trained on a labeled source dataset to a new target dataset using only unlabeled samples from the target. Such a paradigm may not align with real world settings where we are given only a single test instance for adaptation, without having access to any training data. Recently, there has been a pragmatic direction of work namely Test Time Adaptation (TTA) (Sun et al. 2020a; Wang et al. 2021; Khurana et al. 2021), where a model needs to be adapted on the fly, using only a few test samples, with no access to the training data. While these models need multiple test instances to show performance gains, we may not have multiple pages of handwriting for every test writer or style. Hence, we specifically look into the problem of single image test time adaptation for text line recognition models.

Writing style generally varies significantly across individuals, and is often considered as the signature of an individual. For example, some writer's "i" may look like an "l", "n"

Table 1: Comparison of different methods of adaptation. Our TTA setting considers a very challenging realistic scenario where the model has to be adapted to a single handwriting image, without access to any source data, target data or target labels.

Method	Source data		Target Label	Target data			Writer-specific Information
	Few	Many		One	Few	Many	
(Zhang et al. 2019) (Tang et al. 2022) (Kang et al. 2020)		✓				✓	
(Bhunia et al. 2021)	✓		✓	✓			✓
(Kohút, Hradiš, and Kišš 2023)	✓			✓			✓
(Wang and Du 2022)		✓					✓
Ours				✓			

may look like an "r", and so on (Figure 1). However, instead of manually listing all such idiosyncrasies in handwriting across individuals, we would want to develop an algorithm that can automatically learn them on the fly. Typically, one individual’s idiosyncrasies in writing style do not carry over to other individuals. Thus, we do not look into the online paradigm of updating models, but rather reset the model to the source model after every adaptation. This not only saves the model from diverging away, but also avoids any potential privacy concerns (Wang and Kurz 2022).

TTA for image classification and semantic segmentation has been of recent interest in the literature. A few TTA methods (Sun et al. 2020b; Bartler et al. 2022) require access to training data to learn from additional self-supervised losses which can then be optimized for the test instances. Other methods like (Wang et al. 2021; Zhang, Levine, and Finn 2021) do not assume access to source data, but adapt to test data by minimising entropy over a batch where each batch has several data samples. On the contrary, we look into the problem of adapting to one writer style at a time, using only a single test instance. We also do not modify the training strategy, which would otherwise need access to the training data. Moreover, some of the metrics such as entropy used in these works, are non-trivial to compute for text line recognition models specifically for CTC decoder based models, as there can be many mappings to the same output string (Graves et al. 2006).

Existing works on adaptation of text line recognition models require access to lots of unlabeled target data along with labeled source data (Zhang et al. 2019; Tang et al. 2022; Fogel et al. 2020; Kang et al. 2020). But this may not always be possible due to privacy/storage concerns entailing the source data. Other methods like (Bhunia et al. 2021; Kohút, Hradiš, and Kišš 2023) need a few labeled samples of the new writer to adapt the source model. Our method does not need any access to the source data, can be applied on any off-the-shelf text line recognizer, and does not need any labeled data during test-time for adaptation. To the best of our knowledge, TTA from a single handwritten image of a writer, without access to any source data, and without using any writer identification information during source model training, is a novel and more realistic setting which has not been explored yet. Table 1 shows the comparison of different related works in the literature.

Our TTA setting takes as input a single handwritten image

of a writer containing a few lines of handwritten text in it. We look into a de-coupled text-line recognition model consisting of an encoder (optical part) and decoder (language model). Such a model allows us to plug-and-play the language model (LM) based on the domain at hand. Our algorithm exploits both the encoder and the decoder for adaptation. As shown in Figure 2, we first progressively update the optical model using the output from the LM decoder via a weighted CTC loss. The weights are obtained by judging the model’s confidence in a local region around the input image. The iterative nature helps the algorithm to self-improve beyond the original model. We use a computationally efficient character n-gram language model within the loop to get superior quality pseudo-labels than just the optical model’s prediction, which acts as an additional supervisory source. After updating the optical model, which more often looks at local context, we exploit longer context information via a Large Language Model (LLM). Specifically, we get the top-k predictions from the updated model using the beam search algorithm, and then re-rank them based on log-likelihood score of a large language model, which looks at the entire line. We show that both these steps are complementary to each other and offer a significant improvement in performance.

We perform experiments on five benchmark datasets: ICDAR2015-HTR (Sanchez et al. 2015), GNHK (Lee, Chung, and Lee 2021), IAM (Marti and Bunke 2002), CVL (Kleber et al. 2013) and KOHTD (Toiganbayeva et al. 2022). We also create corrupted versions of these datasets similar to (Hendrycks and Dietterich 2019) for image classification, to simulate corruptions which may occur during image acquisition. We perform rigorous qualitative and quantitative experiments, and ablation studies to show the efficacy of the proposed method. The key contributions of this paper are:

1. We introduce the problem of single image test time adaptation for the novel objective of adapting text line recognition to individual styles.
2. We develop an algorithm that uses LM in the loop to update the optical model, followed by refining the predictions by looking at longer context using an LLM.
3. Our algorithm shows significant performance improvements over baselines (Diaz et al. 2021) on multiple datasets.

2 Related Work

Test-Time Adaptation. Test-Time Adaptation (TTA) has been recently studied in the literature for classification (Wang et al. 2021; Bartler et al. 2022; Khurana et al. 2021) and segmentation tasks (Shin et al. 2022; Khurana et al. 2021). These methods can be grouped into two broader categories. First, methods in which the training algorithm includes additional heads for self-supervised tasks (Sun et al. 2020a; Prabhudesai et al. 2022; Bartler et al. 2022). These additional losses are also optimized on the test images during test time. Self-supervised losses include rotation prediction (Sun et al. 2020a), self-reconstruction (Prabhudesai et al. 2022), student-teacher feature prediction

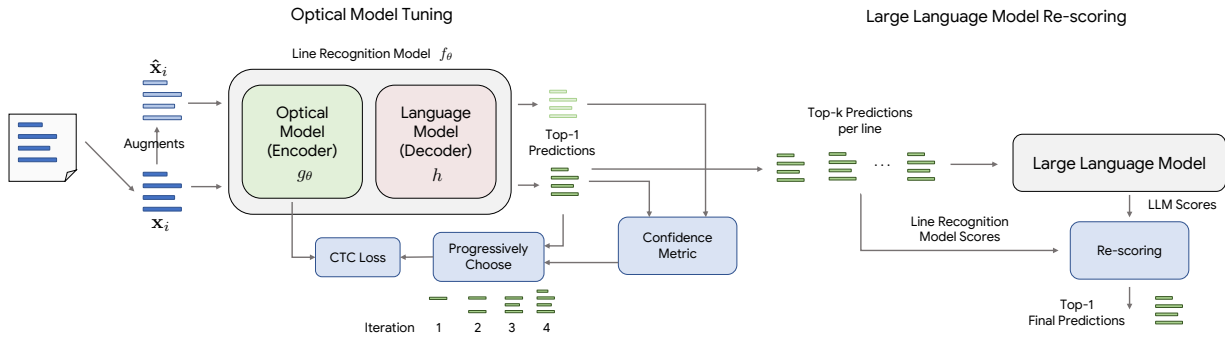


Figure 2: **Framework Overview.** Given an input image, we extract the lines from it. Then pass the original and the augmented version of the lines through the line recognition model which comprises of an optical and a language model. We then compare the outputs for the original and the augmented version of lines to get a confidence measure for each line. Based on this measure, we progressively choose lines and use their self-labels to compute the CTC loss and update the optical model. After updating the optical model in this way, we then extract top-k predictions for every line along with their scores. We then pass these top-k lines through a large language model to obtain the likelihood scores and combine it with the line recognition scores to re-score the top-k predictions and finally predict only the top-1.

(Bartler et al. 2022), etc. The hypothesis is that such losses not only regularize the model during training, but also improve the performance when optimized for test samples, given the gradients for such losses align with the gradients computed w.r.t. the actual labels of the test samples. The second group of methods, on the other hand, do not modify the training strategy and only update the source model using some pseudo-losses such as entropy (Zhang, Levine, and Finn 2021; Wang et al. 2021), self-label cross-entropy (Goyal et al. 2022; Chen et al. 2022), or some specific parameters of the network, such as batch-normalization (Khurana et al. 2021; Hu et al. 2021; Schneider et al. 2020; Nado et al. 2020). Our method falls into the second category where we do not modify the training strategy and do not add any additional head to the network, thus making it applicable to any off-the-shelf text line recognition model.

As these methods are designed for tasks such as classification, it is non-trivial to extend them to sequence learning tasks, which is the focus of this paper. We still adapt some of these methods to the problem at hand, and compare with them in Section 4. Most of these methods do not use any additional source of information beyond the network’s prediction to improve. In this work, we leverage on a language model to improve beyond the optical model’s performance.

Domain Adaptation for Text Line Recognition. Compared to TTA for classification and segmentation tasks where the notion of style is limited, in text line recognition, the notion of style is quite prevalent, as it can vary widely across writers. There have been some works on adaptation of text line recognition models, which can be classified into three broader categories. First, adapting to an entire dataset with a lot of unlabeled samples (Kang et al. 2020; Tang et al. 2022; Fogel et al. 2020; Zhang et al. 2019). Most of the losses and techniques used in such works are analogous to those used in classification and segmentation tasks in literature. The second category of work (Wang and Du 2022; Kohút, Hradiš, and Kišš 2023) assumes access to writer identification information while training the source model, and trains a separate module to extract writer-specific information. Finally,

the third category of work operates in the few shot adaptation technique, assuming access to a few labeled instances for new test writers (Bhunja et al. 2021).

Contrary to aforementioned works, our method does not need access to the source dataset, no information about writers during training, no labeled data for the test writers, and adapts to only one image of handwriting at test time. This makes our model useful for real-world scenarios and applicable to any off-the-shelf model, without making any changes to the model training.

3 Methodology

We first formally define the problem statement, then explain the architecture of the model we use and then describe the proposed approach of test time adaptation.

3.1 Problem Statement

Consider that we are given a text line recognition model, which given an image, predicts the text in it, which is a sequence of characters, i.e., $f_\theta : \mathbf{x} \rightarrow \mathbf{y}$, where $\mathbf{x} \in \mathbb{R}^{h \times w \times 3}$, and $\mathbf{y} \in \mathbb{V}^n$, where \mathbb{V} is vocabulary set of character, and n is variable depending on the model’s prediction.

We consider the problem of test-time adaptation given an image of a page consisting of multiple text lines. We can apply off-the-shelf text line detectors to get a list of text lines $\{\mathbf{x}_i\}_{i=1}^m$. We can then apply the text line recognizer f_θ on the individual lines to get the predicted text. This line recognizer model would generally perform well on handwriting styles that it has seen before, or are similar to such styles. But when encountered with new styles of handwriting, or corruptions on such handwritten images, the model’s performance may degrade. Our objective is to adapt the model f_θ so that it performs better on the test image than the source model. In our setting, after adapting to a test image, we reset the model back to the source model before adapting to a new image.

3.2 Model Architecture

Text line recognition models generally consist of two parts - an encoder, which takes as input a raw image and outputs

features or logits, and a decoder, which produces a sequence of output characters from the features generated by the encoder. The decoder can utilize an explicit language model to encode knowledge about the domain to correct the errors made by the optical model. There are two broad categories of models - end-to-end encoder-decoder models (Li et al. 2021), and de-coupled encoder decoder models trained separately (Diaz et al. 2021). In the latter, the optical model is trained on image data using CTC loss, and the language model is trained on only text data. Typically, the two are combined during inference using scores from both the models. In this work, we use this de-coupled model as the source model, as it is often light-weight, and the de-coupled language model decoder allows a plug-and-play approach for new domains. We follow the self-attention based model architecture of (Diaz et al. 2021). The composite text line recognizer is represented as $f_\theta = h \circ g_\theta$.

Optical Encoder (g_θ) comprises of a convolutional neural network (CNN) like MobileNet (Howard et al. 2017), followed by multiple transformer-like multi-headed self-attention layers (Vaswani et al. 2017) to capture longer range context. Finally, a linear classifier is used to predict the symbols for every frame. The input to this block is $\mathbf{x} \in \mathbb{R}^{h \times w \times 3}$, and the output is logits $g_\theta(\mathbf{x}) \in \mathbb{R}^{w' \times C}$, where w' is a down-sampled version of w , and C is the number of character symbols in the vocabulary. This model is learned using CTC loss (Graves et al. 2006) between the ground-truth label string and the logit.

Language Model Decoder (h) takes in the encoder network’s logits and combines it with the language model to decode text content from it. The decoded string \mathbf{y}^* can be obtained by optimizing the following -

$$\mathbf{y}^* = \arg \max_{\mathbf{y}} p(\mathbf{y}|\mathbf{x})p(\mathbf{y})^\alpha \quad (1)$$

where α is the weight of the language model. It is interesting to note that the formulation of the CTC algorithm (Graves et al. 2006) is such that multiple strings can map to the same final decoded output. An approximate solution to the above problem is obtained by using beam decoding which combines the language model scores, $p(\mathbf{y})$ and optical model scores, $p(\mathbf{y}|\mathbf{x})$ at every step of decoding.

3.3 Test-Time Adaptation

Given an image consisting of multiple lines as input, we want to adapt the model and refine its predictions such that it performs better than when we apply the original source model only. Our adaptation process consists of two parts - updating the optical model, with a computationally efficient language model in the loop (local context), and finally tuning the predictions for every line using a large language model (global context). We next discuss these in detail.

Adapting the Optical Model As discussed before, there are often idiosyncrasies in an individual’s handwriting which are typically consistent. Understanding them would help the model to adapt and personalize the predictions. We develop a self-training mechanism to automatically identify

such idiosyncrasies and update the optical model. It is interesting to note that the optical model alone can make certain errors, which the language model corrects. This acts as a feedback signal to the optical model and improves its performance. However, the confidence of the model can vary across lines, and we would want the model to self-improve by progressively learning from confident lines. We next define the measure of confidence we use in our algorithm.

Confidence of the Optical Model. The predictions of deep neural networks have been often found to be incorrect with high confidence (Nguyen, Yosinski, and Clune 2015). Because of the highly non-linear nature of neural networks, small perturbations in inputs have been shown to have huge differences in outputs (Goodfellow, Shlens, and Szegedy 2014). We hypothesize that smoother transitions in the model’s outputs owing to changes in the input, leads to better correlation between confidence and correctness. In other words, if we perturb the image by a small amount, the predictions should not be perturbed significantly. We use this idea and formalize a measure to assign confidence to every line prediction in the image. This can be formally represented as follows,

$$c(f_\theta(\mathbf{x})) = 1 - d(f_\theta(\mathbf{x}), f_\theta(\hat{\mathbf{x}})) \quad (2)$$

where $\hat{\mathbf{x}}$ is an augmented version of the image \mathbf{x} , and $d()$ can be any distance measure. In our algorithm, we use the normalized edit distance (NED) ($= \text{EditDist}(f_\theta(\mathbf{x}), f_\theta(\hat{\mathbf{x}})) / |f_\theta(\mathbf{x})|$) between the two strings as the distance measure. We use very light augmentations to obtain $\hat{\mathbf{x}}$, as we want to judge local smoothness of the function. More details are discussed in Section 4.

Self-Training Loss. The CTC loss used to train a text line recognizer is at a line level, rather than at a frame level (analogous to pixels in segmentation). Hence, we can only gather self-labels at a line level. Given an image, we first extract the lines from it using any off-the-shelf text line detector (Diaz et al. 2021) to obtain a list of lines $\{\mathbf{x}_i\}_{i=1}^m$. We pass these lines through the encoder and the decoder to obtain self-labels $\{\hat{\mathbf{y}}_i = f_\theta(\mathbf{x}_i)\}_{i=1}^m$. As we only train the optical model using self-training, we can then compute the CTC loss, \mathcal{L}_{CTC} between the self-labels (output of the decoder) and the output of the encoder, i.e., the optical model. Now, as the model may not be equally confident for all lines, we apply the confidence of the model in Eqn 2 to weight the losses. The optimization problem we solve can be represented as follows:

$$\theta^* = \arg \min_{\theta} \sum_{i=1}^m c(f_\theta(\mathbf{x}_i)) \mathcal{L}_{CTC}(g_\theta(\mathbf{x}_i), \hat{\mathbf{y}}_i) \quad (3)$$

Note that all learnable parameters of the network pertain to g_θ , and the above equation optimizes it only. One can also compute the self-labels using just g_θ , i.e., from the optical model’s output itself instead of using the language model incorporated decoder $h \circ g_\theta$. But, we hypothesize that the language model acts as an additional supervisory signal, which helps to improve the performance. We also show that ablation in Section 4. We do not compute any gradients through the confidence function $c()$, but they are updated in every step through forward propagation, as is discussed next.

Progressive Updates. Although we use a confidence measure $c()$ to weight the CTC loss for every line, the confidence metric as well as the self-labels gets better as we adapt. Hence, we progressively update the model starting with high confidence predictions, while updating the self-labels as well as the confidence measure in each iteration. This would allow the model to identify the writer’s style and self-improve, compared to fixing the self-labels and the confidence measure once. We start from the most confident lines, and in each iteration, we keep adding the next most confident ones progressively. Thus, considering we back-propagate for K iterations in total, in the iteration number $k \leq K$, we progressively add $m_k = (k/K)m$ samples, which have the highest values of the confidence metric, to back-propagate and optimize Eqn 3.

Our method to adapt the optical model is shown in Algorithm 1. In each progressive iteration, we first make a forward pass to compute the self-labels \hat{y}_i , and the confidence measure $c(f_\theta(\mathbf{x}_i))$, and then backpropagate only using the fraction of the samples based on the confidence measure. Note that our model learns from self-labels throughout all iterations, and there is a possibility of divergence if the initial predictions turn out to be more incorrect than not. Hence, after adaptation, we compare the final prediction with the initial prediction and if the edit distance between the two is greater than a certain threshold ($=0.75$ used in all experiments), then we use the initial prediction itself.

The above process only updates the encoder, i.e., the optical model. We next discuss how we can tune the predictions using a large language model, instead of the computationally cheap LM used in the decoder, h here.

Algorithm 1: Adapting the Optical Model

Input: Source model: $f_\theta = h \circ g_\theta$, List of lines: $\{\mathbf{x}_i\}_{i=1}^m$

Output: Updated model: $f_\theta = h \circ g_{\theta^*}$

- 1: $\theta_0 \leftarrow \theta$
 - 2: **for** $k = 1 \dots K$ **do**
 - 3: $\hat{\mathbf{x}}_i \leftarrow \text{Augment}(\mathbf{x}_i), \forall i \in [1, m]$
 - 4: // *Forward Propagate*
 - 5: Obtain $f_\theta(\mathbf{x}_i)$ and $f_\theta(\hat{\mathbf{x}}_i) \forall i \in [1, m]$
 - 6: $c(f_\theta(\mathbf{x}_i)) \leftarrow 1 - d(f_\theta(\mathbf{x}_i), f_\theta(\hat{\mathbf{x}}_i)), \forall i \in [1, m]$
 - 7: // *Back Propagate*
 - 8: $\theta_k \leftarrow \theta_{k-1} - \eta \sum_{i \in \text{top-}m_k} c(f_\theta(\mathbf{x}_i)) \nabla_{\theta} \mathcal{L}_{CTC}(g_\theta(\mathbf{x}_i), \hat{\mathbf{y}}_i)$ (4)
 - 9: **end for**
 - 10: $\theta^* \leftarrow \theta_K$
-

Adaptation using a Large Language Model The optical model looks at local context to make a prediction. However, longer length context often helps to correct some of the errors. Large Language Models (LLM) using words tokens instead of characters offers a good mechanism to extract longer context information present in natural text. While an LLM can be used in Eqn 1 itself, that can be computationally expensive. To avoid that, we extract top-k predictions from the CTC decoder $\{\mathbf{y}^i\}_{i=1}^k$, and then re-score the lines using

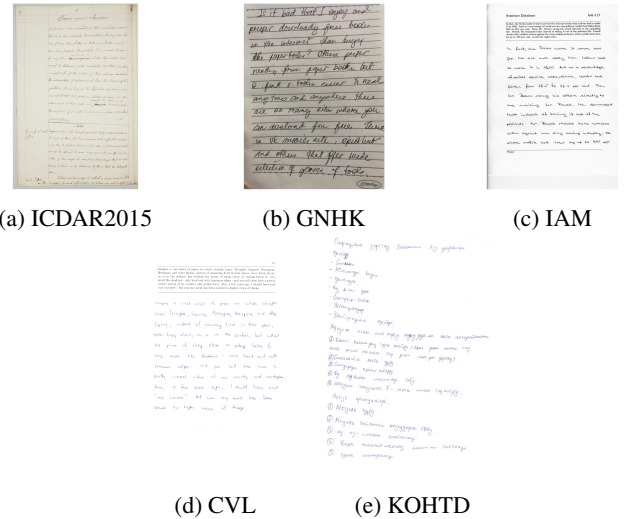


Figure 3: Exemplars from the datasets used in this paper.

an LLM. We use a pre-trained FlanT5-XL model (Chung et al. 2022) as the language model for re-scoring. The log-likelihood score of the LLM can be computed as follows:

$$\mathcal{L}_{LLM} = - \sum_{j=1}^W \log P(\mathbf{w}_j | \mathbf{w}_1, \dots, \mathbf{w}_{j-1}) \quad (5)$$

where \mathbf{w}_i represents the j^{th} word token in a sentence \mathbf{y} . Using only the LLM loss may make it hallucinate, and thus to remain grounded to the actual text in the image, we add the optical score \mathcal{L}_{opt} , which is a combination of the scores from the optical logits and the n-gram LM used in the decoder. Finally, we take a weighted sum of these two scores to pick the best candidate amongst the generated top-k predictions as follows -

$$\text{best_candidate} = \arg \min_i \mathcal{L}_{opt}^i + w * \mathcal{L}_{LLM}^i \quad (6)$$

where w is the weight given to the LLM score, which is a hyper parameter (set to 0.5 for all our experiments).

4 Experiments

To showcase the effectiveness of our method, we perform thorough experimentation and qualitative analysis on five benchmark datasets.

Datasets:

ICDAR2015-HTR (Sanchez et al. 2015) consists of handwritten historical documents in English. This is a particularly challenging dataset due to the variance in writing styles and quality of images. We use the entire dataset of 433 images (train, test, and validation) for testing. We use the split of the dataset which contains line-level annotations.

GoodNotes Handwriting Kollection (GNHK) (Lee, Chung, and Lee 2021) is a handwritten English text dataset, sourced from different regions in the world. It contains various types of texts, like diary notes, shopping lists, etc. captured

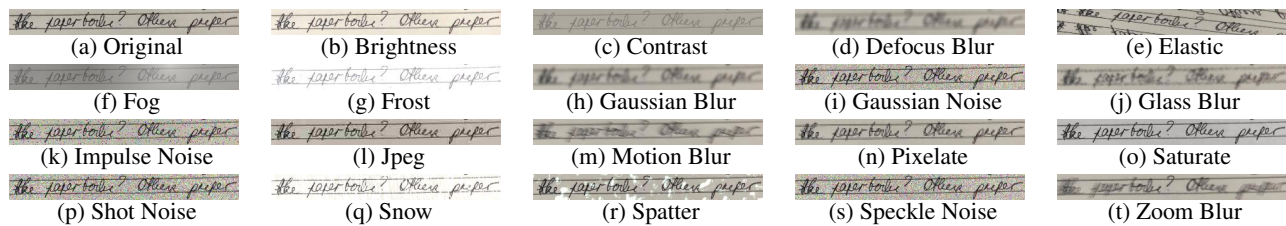


Figure 4: An example original image line and 19 corruptions used from (Hendrycks and Dietterich 2019).

through a mobile phone. This dataset has only word-level annotations, with line ids. We convert that to line annotation by concatenating the word annotations using spaces, and then joining the word images. We use the train and test split consisting of 687 images for evaluation. We omit lines which are printed and have math symbols, as there are no transcriptions for the latter.

IAM Handwriting Database (Marti and Bunke 2002) consists of English handwritten text consisting of 1539 pages from 657 unique writers. The images for this dataset are much clearer than the other datasets and also has line-level annotations. We use the entire dataset for evaluation.

CVL Database (Kleber et al. 2013) consists of English handwritten text consisting of 1598 pages from 7 handwritten texts (1 German and 6 English Texts). 310 writers participated in the dataset. 27 of which wrote 7 texts and 283 writers had to write 5 texts. We use lines from both train and test splits to evaluate the efficacy of our approach.

KOHTD (Toiganbayeva et al. 2022) consists of a large collection of exam papers filled by students in the Kazakh Language (99%) and Russian Language (1%). It contains a total of 1891 images, containing word level annotations for each page. A sample image from each of the datasets is shown in Figure 3.

Corruptions: In real world scenarios, image acquisition generally adds corruptions to the image such as blur, noise, compression, etc. Following (Hendrycks and Dietterich 2019), we create 19 different corrupted versions for each of the five datasets (Figure 4).

Implementation Details: The source model is trained in the same way and on the same datasets as in (Diaz et al. 2021). This model is strong enough as it is trained on lots of labeled and synthetically generated text lines. To calculate the confidence measure for all lines, we augment them using three augmentations, viz, mean filter, median filter and sharpness. Our n-gram model is also similar to (Diaz et al. 2021) ($n = 9$). For test-time adaptation, we use SGD, with a momentum of 0.9, and a learning rate of 10^{-3} . All lines in an image form a single batch of data, to which the model is to be adapted. We follow the same model architecture and configurations as in (Diaz et al. 2021). Only the optical encoder g_θ is adapted to a writer’s handwriting.

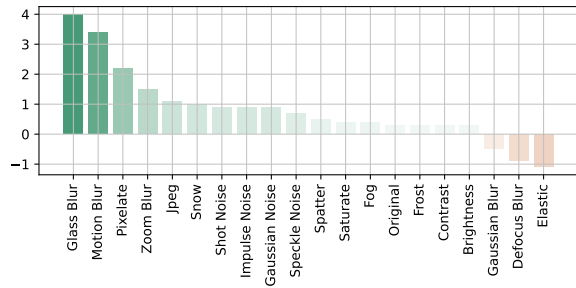
Baselines: To the best of our knowledge, this is the first work on test-time adaptation of text line recognition models from only a single test image, without accessing any source data

Table 2: Performance (CER - lower better) comparison of the proposed method with baselines. “Original” denotes the performance on the non-corrupted dataset and “Corrupted” denotes the average performance over all corruptions. The proposed approach outperforms all, both on original and corrupted versions.

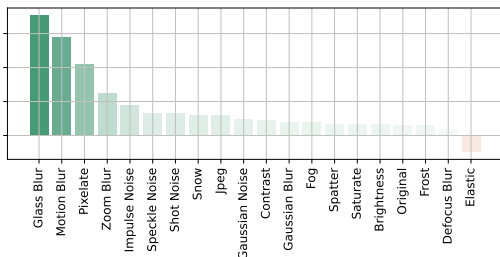
Dataset		Source	BN	PTN	TENT	Ours
IC15-HTR	Original	14.4	17.0	46.8	14.3	13.2
	Corrupted	27.6	30.6	61.6	27.6	25.3
GNHK	Original	14.0	14.2	21.2	14.3	13.3
	Corrupted	24.4	24.2	38.6	25.5	23.0
IAM	Original	6.0	6.1	12.5	6.1	5.4
	Corrupted	15.4	15.1	28.7	15.5	13.8
CVL	Original	8.6	8.7	14.6	8.6	7.7
	Corrupted	26.4	25.8	41.8	26.4	25.9
KOHTD	Original	23.3	23.3	29.4	23.3	16.8
	Corrupted	32.0	31.9	40.8	32.0	25.2

to adapt or without learning any writer identification models while training the source model. As there is no direct baseline in the literature for this use case, we consider three strong baselines from the TTA literature for classification and segmentation, namely BatchNormalization Adaptation (BN) (Schneider et al. 2020), TENT (Wang et al. 2021), and Prediction Time Normalization (PTN) (Nado et al. 2020). These are suited for our problem statement as they do not need any additional changes to the source model training pipeline. While BN and PTN are trivial to extend to this use case, the same is not the case for TENT, which was designed for classification tasks. TENT minimizes the entropy of the predictions by modifying only the affine parameters of the batch normalization layer. As the problem at hand involves a many-to-one mapping from input frames to final sequence, computing the entropy over unique mappings is non-trivial and computationally intractable. Thus, we minimize the mean entropy of all the frames over all lines in the page. We do it for the same number of iterations as in our algorithm.

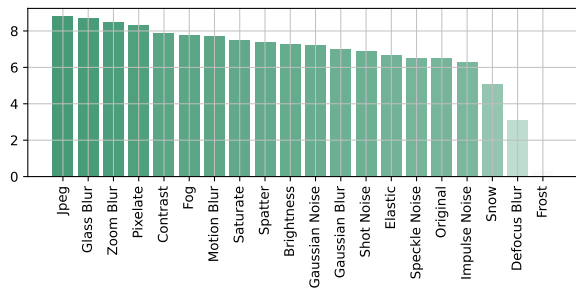
Comparison with baselines: Table 2 shows the performance of our approach compared against the three baselines and the source model. For all the five datasets, the proposed approach outperforms all others. The quantum of improvement is further established when the experiment is repeated on the corrupted versions of the datasets, as shown in Figure 4. The relative improvements across the 19 corrup-



(a) GNHK



(b) IAM



(c) KOHTD

Figure 5: Absolute improvement (in %) obtained with our approach for various corruptions. Apart from minor regressions for a couple of corruption types, the proposed approach shows significant improvement across the board.

tions for two Latin and one non-Latin datasets are shown in Figure 5. Please refer to the appendix for corruption wise improvements. Please note that the original algorithm for TENT uses a batch of more than 100 images, and that too with online updates, i.e., without resetting the model back to the source model after every update, which is what we do in this work. Moreover, we observe that changing the Batch-Norm parameters of the network has a significant impact on the performance. We can see this from the performance of BN which combines the target statistics (mean and variance) with the source statistics using a convex combination. PTN takes this to the extreme by completely replacing the source statistics with the target’s.

Ablation of different choices in self-training: There are several design choices in the proposed self-training algorithm, namely, a) whether to update the self-labels in every learning iteration, b) whether to include the self-labels in the training set progressively instead of taking all of

Table 3: Ablation for self-training algorithm to update the optical model. All methods are trained for the same number of iterations. “NED” here denotes the normalized edit distance, which is the distance function used to compute the confidence measure. All performances are average over 20 datasets (original + 19 corruptions).

Update self-labels	Progressive	Weighting	Confidence		Perf (CER↓)
			CTC	NED	
					26.9
✓					26.6
✓	✓		✓		27.4
✓	✓	✓	✓		25.5
✓	✓			✓	25.3
✓	✓	✓		✓	24.7

the lines at once, c) whether to weight the loss using a confidence metric, and finally d) the confidence measure we use to choose the lines for progressive updates. We conduct an ablation over these choices to observe their individual importance. Table 3 shows this analysis for ICDAR2015-HTR (please refer to appendix for the other datasets). The augmentation based NED metric we use in our algorithm performs better (0.8%) than just using the CTC loss itself as the confidence metric. Moreover, progressive updates lead to **1.6%** improvement than using all of the lines in back-propagation for all iterations.

Ablation of Optical and LLM updates: Our test time adaptation algorithm consists of two parts - adapting the optical model and re-scoring using a large language model. We show an ablation by switching on/off these two blocks in Table 5. The first row represents the source model. As we can see, the optical model updates and LLM re-scoring on their own bring about 2.0% and 0.4% improvement on average over all corruptions, and the composite model outperforms the source model by about **2.2%**.

Ablation of number of iterations: In our approach, if a page has m lines, we progressively add m/K lines based on the confidence metric rank in each iteration, where K is the total number of progressive update iterations. In all our experiments over all datasets, we use $K = 4$. Figure 6 shows the variations in performance for different values of K . The performance variations are more apparent for corruptions where the performance is low. If too few updates are used, then there is less scope for improvement through self-labeling. On the other hand, if too many rounds of updates are performed, model outputs tend to diverge, effectively over-fitting to inaccurate self-labeled data.

What are the changes that the model makes?: Moreover, we analyze the changes in character predictions, the model makes that leads to improvement in performance. We create a list of all replacement edits between the ground-truth and the source model predictions, as well as between the ground-truth and the TTA adapted model. We then look at the replacements which are not there in the second list, but there in the first list. We analyze this on the ICDAR2015-HTR dataset and present the most frequent replacements in

Table 4: Most frequent character replacements made by our TTA algorithm that lead to a better performance.

Before	<i>o</i>	<i>l</i>	<i>a</i>	<i>a</i>	<i>n</i>	<i>e</i>	<i>i</i>	<i>m</i>	<i>e</i>	<i>e</i>	<i>T</i>	<i>a</i>	<i>n</i>	<i>u</i>	<i>a</i>	<i>s</i>	<i>o</i>	<i>d</i>	<i>e</i>	<i>r</i>
After	<i>e</i>	<i>t</i>	<i>o</i>	<i>e</i>	<i>r</i>	<i>o</i>	<i>e</i>	<i>n</i>	<i>i</i>	<i>a</i>	<i>t</i>	<i>u</i>	<i>e</i>	<i>e</i>	<i>r</i>	<i>e</i>	<i>a</i>	<i>t</i>	<i>s</i>	<i>n</i>
Count	182	155	151	150	149	135	122	108	103	93	92	91	87	87	84	82	80	80	80	78

Table 5: Importance of updating the optical model, and/or re-scoring the final outputs using an LLM. All performances are average over 20 datasets (original + 19 corruptions).

Optical Updates	LLM Rescoring	Perf (CER↓)
		26.9
	✓	26.5
✓		24.9
✓	✓	24.7

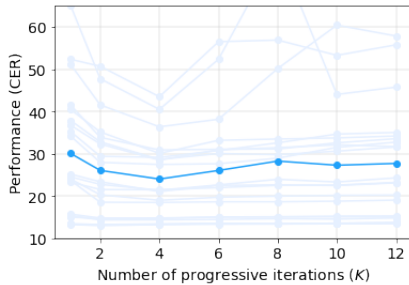


Figure 6: **Performance variation for different number of updates.** Each line shows the performance for one corruption. The average performance is highlighted in the darker shade.

Table 4. Most replacements occur among similar looking characters and our TTA algorithm is able to figure them out on the fly.

The role of LM in adapting the optical model: As shown in Figure 2, our TTA algorithm includes the language model in the loop to update the optical model. This plays an interesting role, compared to other works in TTA which do not use any extra information. As the model is updated using self-training, it can often diverge because of incorrect self-labels. However, the LM acts as a correction module, preventing accidental divergence. We performed an experiment without LM in our TTA algorithm and observed a CER of 29.5% averaged over all corruptions on GNHK, compared to 23.9% when LM is used in TTA. We also plot the performance improvement of the source model with and without using LM in the decoder vs the performance difference with and without using LM in TTA (Figure 7). It shows that for corruptions where using LM in decoding offers higher improvement for source model’s inference, using LM in TTA shows even greater improvement compared to TTA without LM. This is interesting and further highlights the importance of using LM in TTA particularly when the optical model is more confused.

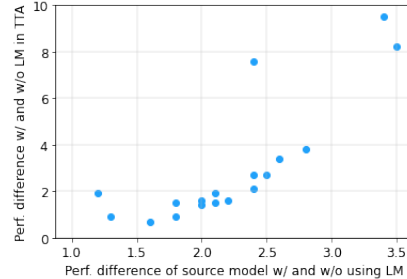


Figure 7: **The role of LM in adapting the optical model.** Each point here denotes the relative improvement the LM introduces for various corrupted versions of the GNHK dataset. The x value of each point is the CER improvement when decoding is done using the LM Decoder vs GreedyDecoder when evaluating the source model. The y-axis shows the CER improvement when our proposed method is used with the LM Decoder vs GreedyDecoder.

5 Conclusion

We introduce the problem of adapting text line recognition models to specific writers using a single test image, without accessing any labeled source data. We develop a method that first progressively adapts the optical model, using an augmentation based confidence function (local context). We further tune the predictions using an LLM which looks at the context of the entire line. Through rigorous experiments and ablation studies on five benchmark datasets, we establish the efficacy of our method.

References

- Bartler, A.; Bühler, A.; Wiewel, F.; Döbler, M.; and Yang, B. 2022. Mt3: Meta test-time training for self-supervised test-time adaptation. In *AISTATS*, 3080–3090. PMLR.
- Bhunia, A.; Ghose, S.; Kumar, A.; Chowdhury, P.; Sain, A.; and Song, Y. 2021. MetaHTR: Towards Writer-Adaptive Handwritten Text Recognition. In *2021 IEEE/CVF Conference on Computer Vision and Pattern Recognition (CVPR)*, 15825–15834. Los Alamitos, CA, USA: IEEE Computer Society.
- Bhunia, A. K.; Das, A.; Bhunia, A. K.; Kishore, P. S. R.; and Roy, P. P. 2019. Handwriting Recognition in Low-Resource Scripts Using Adversarial Learning. In *2019 IEEE/CVF Conference on Computer Vision and Pattern Recognition (CVPR)*, 4762–4771.
- Breuel, T. M.; Ul-Hasan, A.; Al-Azawi, M. A.; and Shafait, F. 2013. High-performance OCR for printed English and Fraktur using LSTM networks. In *ICDAR*, 683–687. IEEE.
- Chen, D.; Wang, D.; Darrell, T.; and Ebrahimi, S. 2022. Contrastive test-time adaptation. In *CVPR*, 295–305.
- Chung, H. W.; Hou, L.; Longpre, S.; Zoph, B.; Tay, Y.; Fedus, W.; Li, E.; Wang, X.; Dehghani, M.; Brahma, S.; et al. 2022. Scaling instruction-finetuned language models. *arXiv preprint arXiv:2210.11416*.
- Diaz, D. H.; Qin, S.; Ingle, R. R.; Fujii, Y.; and Bissacco, A. 2021. Rethinking Text Line Recognition Models. *ArXiv*, abs/2104.07787.
- Fogel, S.; Averbuch-Elor, H.; Cohen, S.; Mazor, S.; and Litman, R. 2020. ScrabbleGAN: Semi-Supervised Varying Length Handwritten Text Generation. *2020 IEEE/CVF Conference on Computer Vision and Pattern Recognition (CVPR)*, 4323–4332.
- Goodfellow, I. J.; Shlens, J.; and Szegedy, C. 2014. Explaining and harnessing adversarial examples. *arXiv preprint arXiv:1412.6572*.
- Goyal, S.; Sun, M.; Raghunathan, A.; and Kolter, Z. 2022. Test-time adaptation via conjugate pseudo-labels. *NeurIPS*.
- Graves, A.; Fernández, S.; Gomez, F.; and Schmidhuber, J. 2006. Connectionist temporal classification: labelling unsegmented sequence data with recurrent neural networks. In *Proceedings of the 23rd international conference on Machine learning*, 369–376.
- Hendrycks, D.; and Dietterich, T. 2019. Benchmarking neural network robustness to common corruptions and perturbations. *ICLR*.
- Hoffman, J.; Tzeng, E.; Park, T.; Zhu, J.-Y.; Isola, P.; Saenko, K.; Efros, A.; and Darrell, T. 2018. Cycada: Cycle-consistent adversarial domain adaptation. In *ICML*. Pmlr.
- Howard, A. G.; Zhu, M.; Chen, B.; Kalenichenko, D.; Wang, W.; Weyand, T.; Andreetto, M.; and Adam, H. 2017. MobileNets: Efficient Convolutional Neural Networks for Mobile Vision Applications. *ArXiv*, abs/1704.04861.
- Hu, X.; Uzunbas, G.; Chen, S.; Wang, R.; Shah, A.; Nevatia, R.; and Lim, S.-N. 2021. Mixnorm: Test-time adaptation through online normalization estimation. *arXiv preprint arXiv:2110.11478*.
- Ingle, R. R.; Fujii, Y.; Deselaers, T.; Baccash, J.; and Papat, A. C. 2019. A scalable handwritten text recognition system. In *2019 International Conference on Document Analysis and Recognition (ICDAR)*, 17–24. IEEE.
- Kang, L.; Rusiñol, M.; Fornés, A.; Riba, P.; and Villegas, M. 2020. Unsupervised Adaptation for Synthetic-to-Real Handwritten Word Recognition. In *2020 IEEE Winter Conference on Applications of Computer Vision (WACV)*, 3491–3500.
- Khurana, A.; Paul, S.; Rai, P.; Biswas, S.; and Aggarwal, G. 2021. Sita: Single image test-time adaptation. *CVPR-W*.
- Kleber, F.; Fiel, S.; Diem, M.; and Sablatnig, R. 2013. CvI-database: An off-line database for writer retrieval, writer identification and word spotting. In *ICDAR*, 560–564. IEEE.
- Kohút, J.; Hradiš, M.; and Kišš, M. 2023. Towards Writing Style Adaptation in Handwriting Recognition. *arXiv preprint arXiv:2302.06318*.
- Lee, A. W. C.; Chung, J.; and Lee, M. 2021. GNHK: A Dataset for English Handwriting in the Wild. In *International Conference of Document Analysis and Recognition (ICDAR)*.
- Li, M.; Lv, T.; Chen, J.; Cui, L.; Lu, Y.; Florencio, D.; Zhang, C.; Li, Z.; and Wei, F. 2021. Trocr: Transformer-based optical character recognition with pre-trained models. *arXiv preprint arXiv:2109.10282*.
- Long, S.; He, X.; and Yao, C. 2021. Scene text detection and recognition: The deep learning era. *IJCV*, 129: 161–184.
- Marti, U.-V.; and Bunke, H. 2002. The IAM-database: an English sentence database for offline handwriting recognition. *International Journal on Document Analysis and Recognition*, 5: 39–46.
- Nado, Z.; Padhy, S.; Sculley, D.; D’Amour, A.; Lakshminarayanan, B.; and Snoek, J. 2020. Evaluating prediction-time batch normalization for robustness under covariate shift. *arXiv preprint arXiv:2006.10963*.
- Nguyen, A.; Yosinski, J.; and Clune, J. 2015. Deep neural networks are easily fooled: High confidence predictions for unrecognizable images. In *CVPR*, 427–436.
- Prabhudesai, M.; Paul, S.; van Steenkiste, S.; Sajjadi, M. S.; Goyal, A.; Pathak, D.; Fragkiadaki, K.; Aggarwal, G.; and Kipf, T. 2022. Test-time adaptation with slot-centric models. In *NeurIPS Workshop*.
- Sanchez, J. A.; Toselli, A. H.; Romero, V.; and Vidal, E. 2015. ICDAR 2015 competition HTRtS: Handwritten Text Recognition on the tranScriptorium dataset. In *ICDAR*, 1166–1170. IEEE.
- Schneider, S.; Rusak, E.; Eck, L.; Bringmann, O.; Brendel, W.; and Bethge, M. 2020. Improving Robustness against Common Corruptions by Covariate Shift Adaptation. In *Proceedings of the 34th International Conference on Neural Information Processing Systems, NIPS’20*. Red Hook, NY, USA: Curran Associates Inc. ISBN 9781713829546.
- Shin, I.; Tsai, Y.-H.; Zhuang, B.; Schuster, S.; Liu, B.; Garg, S.; Kweon, I. S.; and Yoon, K.-J. 2022. MM-TTA: multi-modal test-time adaptation for 3d semantic segmentation. In *CVPR*, 16928–16937.

Sun, Y.; Wang, X.; Liu, Z.; Miller, J.; Efros, A.; and Hardt, M. 2020a. Test-time training with self-supervision for generalization under distribution shifts. In *ICML*, 9229–9248. PMLR.

Sun, Y.; Wang, X.; Zhuang, L.; Miller, J.; Hardt, M.; and Efros, A. A. 2020b. Test-Time Training with Self-Supervision for Generalization under Distribution Shifts. In *ICML*.

Tang, P.; Peng, L.; Yan, R.; Shi, H.; Yao, G.; Liu, C.; Li, J.; and Zhang, Y. 2022. Domain Adaptation via Mutual Information Maximization for Handwriting Recognition. In *ICASSP 2022-2022 IEEE International Conference on Acoustics, Speech and Signal Processing (ICASSP)*, 2300–2304. IEEE.

Toiganbayeva, N.; Kasem, M.; Abdimanap, G.; Bostanbekov, K.; Abdallah, A.; Alimova, A.; and Nurseitov, D. 2022. KOHTD: Kazakh offline handwritten text dataset. *SPIC*, 116827.

Tsai, Y.-H.; Hung, W.-C.; Schuler, S.; Sohn, K.; Yang, M.-H.; and Chandraker, M. 2018. Learning to adapt structured output space for semantic segmentation. In *Proceedings of the IEEE conference on computer vision and pattern recognition*, 7472–7481.

Vaswani, A.; Shazeer, N. M.; Parmar, N.; Uszkoreit, J.; Jones, L.; Gomez, A. N.; Kaiser, L.; and Polosukhin, I. 2017. Attention is All you Need. *ArXiv*, abs/1706.03762.

Wang, D.; Shelhamer, E.; Liu, S.; Olshausen, B.; and Darrell, T. 2021. Tent: Fully Test-Time Adaptation by Entropy Minimization. In *International Conference on Learning Representations*.

Wang, Q.; and Kurz, D. 2022. Reconstructing training data from diverse ml models by ensemble inversion. In *WACV*, 2909–2917.

Wang, Z.-R.; and Du, J. 2022. Fast writer adaptation with style extractor network for handwritten text recognition. *Neural Networks*.

Zhang, M.; Levine, S.; and Finn, C. 2021. MEMO: Test Time Robustness via Adaptation and Augmentation. *NeurIPS*.

Zhang, Y.; Nie, S.; Liu, W.; Xu, X.; Zhang, D.; and Shen, H. T. 2019. Sequence-To-Sequence Domain Adaptation Network for Robust Text Image Recognition. In *2019 IEEE/CVF Conference on Computer Vision and Pattern Recognition (CVPR)*, 2735–2744.

Appendix

A Exemplars of predictions over progressive self-training iterations

Figure 8 shows the predictions after every iteration of the proposed self-training approach. As we can see, the predictions improve over iterations. For example, for the second one from top, the model quickly figures out that the style of ‘l’ looks different from that of ‘d’, and hence it corrects that in the later iterations. Similarly for the third example from the top, the multiple ‘s’ in “session” get correctly recognized over iterations. We see similar improvements in the other examples as well.

B Category-wise ablation of self-training the optical model

In Tables 6, 7, 8, 9 and 10, we show ablation results for various choices of our self-training approach. For ICDAR2015-HTR, we observe that our method performs better than the other options for most corruptions. Our augmentation based reweighting strategy with progressive update of labels shows CER improvements of as much as **5.6%** (for impulse noise corruption).

For the GNHK dataset, we observe similar trends as ICDAR2015-HTR. We observe an improvement in CER of as much as **4.7%** for the glass blur corruption. On an average, our proposed augmentation based TTA with reweighting performs the best and shows an improvement of 1.3% over the baseline for all corruptions, including the original dataset.

In case of IAM, we observe that our method performs much better than the other options on average. Our method perform the best for majority of the corruptions, and shows an improvement of as much as **7.1%** (for the glass blur corruption). For a few of the corruptions adapting the model using predictions over all lines of an image as pseudo labels helps better. We speculate this happens because IAM being a much easier dataset, the predictions generated from the source model itself are of good quality, and hence serve as good self-labels. Thus, updating the model with the self-labels for all lines, over all iterations performs a bit better.

For the CVL dataset, we observe improvements in most cases, with a maximum improvement of **5.5%**, except a few corruptions like defocus_blur, elastic, gaussian_blur and zoom_blur. This can be attributed to the correctness of the self-labels due to the hard inherent distortions these corruptions introduce.

In case of the dataset, KOHTD, we observe a consistent improvement across all corruptions. We observe that our progressive update of self-labels with reweighting shows CER improvements of at least 0.3% and as much as **8.8%**. KOHTD, being a low resource language dataset, we believe that the divergence controlled adaptation we introduce helps identify and learn from the writer’s idiosyncrasies very effectively.

C Understanding the correlation between our confidence metric and correctness.

In our algorithm, we use a confidence metric to both rank and weight losses for lines – which forms the core of our progressive self-training approach. Our confidence metric (which we call the Normalized Edit Distance (NED) in the tables and figures) determines whether the optical model is smooth in the neighborhood of the input image. A baseline confidence metric is the CTC loss itself w.r.t. the top-1 prediction, with which we compare in Tables 6, 7, 8, 9 and 10. In order to better understand the usefulness of the proposed confidence metric, we find the correlation of the confidence metric and the CER of the self-labels with the ground-truth. We perform the analysis for both our metric and the CTC loss based weights (normalized over all lines in an image). The plots over the five datasets are shown in Figures 9, 10, 11, 12 and 13. As we can see from the plots on the right of the figures which represent the confidence scores derived using our augmentation based NED metric, as the CER for a line increases, the confidence of the model over the line also decreases. We see a much higher correlation between the CER and the proposed metric than the confidence based on the CTC loss.

D Ablation studies with varying number of iterations

We evaluate our method for different number of iterations K of our self-training algorithm. Recall, we progressively add $\frac{m}{K}$ lines to our set of confident lines, where m is the total number of lines in an image. We run our algorithm for $K \in \{1, 2, 4, 6, 8, 10, 12\}$. The results are shown for all corruptions in tables 11, 12, 13, 14 and 15. As discussed in the paper, when we have very few update iterations, we do not allow the self-training algorithm to improve, and on the other hand, too many iterations may lead to divergence, as the algorithm does not use any ground-truth labels, but learns from self-labels only. We find that for all the datasets, number of iterations $K = 4$, i.e., incrementally taking 25% of the lines in each iteration results in the best performance. We can observe that choosing $K = 4$ helps us strike the right balance between performance and total number of iterations.

E The Impact of LM on TTA

In the paper we show this analysis on GNHK, where we find that the performance significantly degrades if we do not use the LM in the self-training loop. This is because the LM acts as a cushion and prevents the model from diverging, which can otherwise happen because of the incorrect self-labels from just the optical model. Here, we show the analysis on two other datasets. When we do not use LM in the self-training algorithm, we observe a drop in performance from 23.9 to 44.4 on ICDAR2015-HTR, from 24.7 to 31.4 on GNHK, and from 13.6 to 21 on IAM. We also show a similar plot as in the paper in Figure 14 for ICDAR2015-HTR and IAM. The plot shows how the performance improvement offered by the LM on the source model inference can have an impact on the TTA performance.

			Confidence		Performance																	AVERAGE			
Update self-labels	Progressive	Weighting	CTC	NED	original	brightness	contrast	defocus blur	elastic	fog	frost	gaussian blur	gaussian noise	glass blur	impulse noise	jpeg	motion blur	pixelate	saturate	shot noise	snow		spatter	speckle noise	zoom blur
✓					14.4	14.3	15.6	39.2	42.7	16.2	29.6	19.9	26.3	35.5	36.9	27.0	31.0	26.2	14.4	35.8	23.3	15.9	37.9	36.4	26.9
✓					13.3	13.2	14.1	40.0	42.8	15.7	28.8	18.1	23.6	31.3	32.2	23.2	27.6	20.9	13.7	32.3	21.8	14.7	34.8	36.3	24.9
✓	✓		✓		13.5	13.5	14.7	39.8	43.5	15.2	29.4	18.8	24.0	32.1	33.1	23.7	28.5	21.5	13.5	32.8	22.0	15.0	35.3	36.8	25.3
✓	✓				13.5	13.4	14.7	39.1	47.2	15.2	29.3	18.6	24.0	32.1	32.9	23.7	28.6	21.3	13.5	33.0	21.8	15.0	35.1	37.4	25.5
✓	✓			✓	13.3	13.2	14.5	38.9	43.4	15.1	28.8	18.4	23.4	30.5	31.9	23.0	28.0	20.7	13.3	31.8	21.7	14.8	33.8	37.3	24.8
✓	✓	✓		✓	13.2	13.0	14.2	39.1	46.8	14.9	28.4	18.2	22.8	30.5	31.3	22.6	27.9	20.1	13.1	31.4	21.0	14.6	33.4	37.0	24.7

Table 6: Ablation results for different setting of self-training to update the optical model. The results are on ICDAR2015-HTR.

			Confidence		Performance																	AVERAGE			
Update self-labels	Progressive	Weighting	CTC	NED	original	brightness	contrast	defocus blur	elastic	fog	frost	gaussian blur	gaussian noise	glass blur	impulse noise	jpeg	motion blur	pixelate	saturate	shot noise	snow		spatter	speckle noise	zoom blur
✓					14.0	14.5	15.8	30.2	56.9	17.3	21.2	22.1	20.1	38.4	22.6	18.4	33.5	20.2	14.6	22.7	26.1	18.9	19.8	29.7	23.8
✓					13.9	14.1	15.4	30.8	57.5	16.9	20.8	22.4	19.3	35.2	21.8	17.2	30.3	18.4	14.4	22.0	25.0	18.4	19.1	29.3	23.1
✓	✓		✓		13.9	14.3	16.3	31.6	58.4	17.1	24.2	28.8	19.5	35.2	22.3	17.5	30.6	18.5	14.4	22.3	25.3	18.5	19.1	28.9	23.8
✓	✓				13.9	14.3	15.7	31.6	58.3	17.2	20.9	23.0	19.5	34.8	21.9	17.5	30.7	18.5	14.4	22.0	25.0	18.5	19.2	28.6	23.3
✓	✓			✓	13.8	14.2	15.6	31.0	58.1	16.9	20.9	22.6	19.2	34.5	21.6	17.2	30.0	18.0	14.2	22.9	25.0	18.4	19.0	30.6	23.2
✓	✓	✓		✓	13.3	13.8	15.1	30.7	58.1	16.4	20.4	22.2	18.8	33.7	21.1	16.7	29.7	17.5	13.7	21.3	24.2	17.8	18.5	28.0	22.6

Table 7: Ablation results for different setting of self-training to update the optical model. The results are on GNHK.

			Confidence		Performance																	AVERAGE			
Update self-labels	Progressive	Weighting	CTC	NED	original	brightness	contrast	defocus blur	elastic	fog	frost	gaussian blur	gaussian noise	glass blur	impulse noise	jpeg	motion blur	pixelate	saturate	shot noise	snow		spatter	speckle noise	zoom blur
✓					6.0	7.1	7.1	20.1	57.7	6.8	11.5	13.2	7.4	26.3	11.8	7.6	22.4	12.2	6.1	9.4	13.7	6.7	9.1	38.1	15.0
✓					5.7	6.6	6.4	19.9	58.6	6.2	11.1	12.4	6.8	19.5	10.6	6.9	16.7	8.6	5.8	8.6	12.8	6.3	8.4	38.3	13.8
✓	✓		✓		5.9	6.8	6.9	20.0	57.7	6.3	11.0	13.2	7.3	26.2	11.2	7.0	18.2	8.5	5.8	8.8	12.9	6.5	8.4	38.0	14.3
✓	✓				5.8	6.8	6.7	20.7	59.5	6.5	11.5	13.2	7.0	20.1	10.7	7.1	17.7	8.9	5.9	8.9	13.2	6.5	8.6	38.5	14.2
✓	✓			✓	5.7	6.6	6.5	19.9	59.1	6.1	11.2	12.7	6.9	19.9	10.2	6.8	16.9	8.5	5.7	8.8	12.9	6.3	8.3	37.5	13.8
✓	✓	✓		✓	5.4	6.4	6.2	19.7	58.7	5.9	10.9	12.4	6.4	19.2	9.9	6.4	16.6	8.0	5.4	8.0	12.5	5.9	7.9	35.6	13.4

Table 8: Ablation results for different setting of self-training to update the optical model. The results are on IAM.

			Confidence		Performance																	AVERAGE			
Update self-labels	Progressive	Weighting	CTC	NED	original	brightness	contrast	defocus blur	elastic	fog	frost	gaussian blur	gaussian noise	glass blur	impulse noise	jpeg	motion blur	pixelate	saturate	shot noise	snow		spatter	speckle noise	zoom blur
✓					8.6	11.0	12.6	30.4	59.0	11.5	37.0	20.6	15.4	34.1	27.9	14.7	35.8	16.6	12.9	26.4	51.8	11.5	26.6	46.6	25.5
✓					8.1	10.6	12.0	37.3	62.4	11.0	48.7	24.2	18.8	28.8	25.6	13.1	30.6	13.3	12.7	23.1	51.8	11.1	23.6	52.9	26.0
✓	✓		✓		8.5	10.9	12.4	34.7	61.8	11.4	39.7	24.0	14.8	29.6	25.8	13.3	31.1	13.6	13.6	24.8	53.4	11.3	25.3	55.1	25.8
✓	✓				8.5	11.3	12.5	35.7	62.6	11.4	39.7	23.7	14.9	29.6	26.4	13.3	31.0	13.8	13.3	25.0	53.2	11.4	25.4	57.4	26.0
✓	✓			✓	8.3	10.7	12.2	34.4	61.4	11.1	39.4	23.3	14.5	29.4	25.4	13.0	30.4	13.1	13.3	24.4	53.6	11.2	24.9	55.4	25.5
✓	✓	✓		✓	7.8	10.2	11.5	33.8	61.5	10.5	39.0	22.8	13.9	29.1	24.8	12.3	30.3	12.4	12.6	23.9	53.4	10.5	24.4	56.2	25.0

Table 9: Ablation for different setting of self-training to update the optical model. The results are on CVL.

			Confidence		Performance																	AVERAGE			
Update self-labels	Progressive	Weighting	CTC	NED	original	brightness	contrast	defocus blur	elastic	fog	frost	gaussian blur	gaussian noise	glass blur	impulse noise	jpeg	motion blur	pixelate	saturate	shot noise	snow		spatter	speckle noise	zoom blur
✓					23.3	27.2	27.9	36.5	29.0	31.8	55.2	26.9	26.9	31.5	33.8	29.1	39.0	27.0	24.9	30.1	43.5	25.0	31.8	30.5	31.5
✓					20.1	24.2	24.7	36.2	28.6	31.8	56.4	23.9	23.8	25.4	29.2	29.1	34.0	27.0	21.9	27.4	41.2	22.6	25.4	30.1	28.8
✓	✓		✓		20.3	24.7	25.2	32.6	27.3	31.9	56.7	23.9	26.1	25.8	29.2	28.6	33.1	26.6	19.7	28.3	39.3	22.3	27.2	32.1	29.0
✓	✓				20.7	24.9	25.5	25.4	27.5	31.9	56.9	23.5	26.1	25.6	28.9	28.6	33.2	26.3	19.2	28.1	39.2	22.5	27.2	32.8	29.0
✓	✓			✓	18.7	21.5	22.7	34.4	27.5	26.9	55.7	20.3	23.1	25.6	27.8	23.5	33.2	20.5	18.8	18.3	39.0	20.4	26.1	25.6	26.8
✓	✓	✓		✓	16.8	19.9	20.1	33.4	22.3	24.0	54.8	19.9	19.7	22.7	27.6	20.3	31.3	18.7	17.4	23.1	38.5	17.7	25.3	22.1	24.8

Table 10: Ablation for different setting of self-training to update the optical model. The results are on KOHTD.

	Number of Iterations						
	1	2	4	6	8	10	12
original	13.5	13.3	13.3	13.4	13.6	13.6	13.8
brightness	13.4	13.2	13.2	13.4	13.5	13.5	13.8
contrast	15.5	14.6	14.5	14.7	14.8	14.8	15.1
defocus blur	49.8	43.6	39.1	38.4	38.4	38.0	38.1
elastic	48.0	46.6	46.3	43.3	43.2	43.5	43.9
fog	15.8	14.9	15.1	15.3	15.4	15.5	15.6
frost	33.9	29.0	28.6	28.9	29.0	29.0	29.5
gaussian blur	23.2	18.8	18.5	18.7	18.9	18.7	19.1
gaussian noise	24.8	23.5	23.2	23.6	23.7	23.7	23.9
glass blur	37.2	33.0	30.5	30.4	30.5	30.5	30.9
impulse noise	40.5	34.3	31.9	31.4	31.9	32.0	32.7
jpeg	25.7	23.9	23.1	23.1	23.1	23.1	23.2
motion blur	34.2	28.5	28.1	28.3	29.5	28.2	28.4
pixelate	24.9	21.5	20.8	21.0	21.1	21.2	23.8
saturate	13.5	13.3	13.3	13.4	13.5	13.6	13.8
shot noise	36.7	33.0	32.0	31.8	32.1	32.2	32.1
snow	23.4	21.8	21.6	21.9	22.2	22.1	22.5
spatter	15.1	14.8	14.8	15.0	15.1	15.1	15.3
speckle noise	39.7	35.4	33.9	33.7	33.8	34.1	34.1
zoom blur	47.3	40.1	36.9	36.1	36.5	36.8	36.5
AVERAGE	28.8	25.9	24.9	24.8	25.0	25.0	25.3

Table 11: Performance variation (on ICDAR2015-HTR) for different number of progressive updates. For Number of Iterations = K , the algorithm is run for K iterations, with $\frac{100}{K}k\%$ of top lines included in the self-training algorithm for iteration number $k \in [1, K]$. As we

F Writer-specific Adaptation

Most of the datasets considered here, and in practice as well, generally consist of only lines from one writer, and thus one writing style. This helps the algorithm to learn from multiple cues across lines, and adapt to the writer’s style. This becomes difficult when the same page has writing from multiple writers, as then the number of lines per writer decreases. To do this experiment, we concoct a dataset, where we create pages (i.e., list of lines) by randomly choosing lines from multiple pages (from different writers), without replacement. Then we run our TTA algorithm, except that now it sees lines from multiple writers at a time in a page. We present the performances in Figure 15 for all the datasets. The x-axis and y-axis show the performance on the vanilla and concocted dataset. As we can see almost all the points lie above the equi-performance line, indicating that single writer specific adaptation works much better than having multiple writers in a single page.

	Number of Iterations						
	1	2	4	6	8	10	12
original	13.9	13.9	13.7	13.8	13.9	13.9	13.9
brightness	14.2	14.1	14.2	14.2	14.3	14.3	14.3
contrast	15.7	15.6	15.5	15.6	15.6	15.6	15.8
defocus blur	32.7	30.9	31.0	31.1	30.9	30.9	30.9
elastic	57.5	58.2	58.0	57.7	57.8	57.8	57.7
fog	17.0	17.0	16.9	17.1	17.1	17.3	17.2
frost	20.8	20.8	20.9	20.9	21.1	21.1	21.2
gaussian blur	23.6	22.6	22.7	22.8	22.8	22.8	22.8
gaussian noise	19.7	19.4	19.3	19.3	19.4	19.4	19.4
glass blur	37.1	34.9	34.4	34.6	34.7	34.6	34.7
impulse noise	22.1	21.6	21.7	21.6	21.7	21.7	21.7
jpeg	17.3	17.1	17.3	17.2	17.0	17.3	17.2
motion blur	30.4	29.8	30.1	30.3	30.5	30.7	30.9
pixelate	18.8	18.2	18.0	18.0	18.1	18.3	18.1
saturate	14.4	14.3	14.2	14.3	14.3	14.4	14.3
shot noise	22.3	21.9	21.8	21.8	21.6	21.6	21.8
snow	25.0	25.0	25.0	25.1	25.3	25.3	25.4
spatter	18.4	18.4	18.4	18.5	18.5	18.4	18.5
speckle noise	19.3	19.0	19.1	19.0	18.9	19.0	19.1
zoom blur	31.5	28.7	28.2	28.0	28.1	28.3	28.1
AVERAGE	23.6	23.1	23.0	23.0	23.1	23.1	23.2

Table 12: Performance variation (on GNHK) for different number of progressive updates. For Number of Iterations = K , the algorithm is run for K iterations, with $\frac{100}{K}k\%$ of top lines included in the self-training algorithm for iteration number $k \in [1, K]$.

	Number of Iterations						
	1	2	4	6	8	10	12
original	5.8	5.8	5.8	5.8	5.8	5.8	5.8
brightness	7.0	6.8	6.8	6.8	6.8	6.8	6.9
contrast	7.5	6.6	6.6	6.6	6.7	6.6	6.7
defocus blur	24.0	20.4	20.2	20.5	20.6	20.4	20.5
elastic	59.0	59.1	58.7	58.4	58.3	58.5	58.2
fog	6.5	6.4	6.3	6.4	6.4	6.4	6.4
frost	12.5	11.4	11.3	11.6	11.8	11.7	11.8
gaussian blur	14.7	12.8	12.9	13.0	13.1	13.0	13.1
gaussian noise	7.0	6.9	6.8	6.9	6.9	6.9	6.9
glass blur	26.9	21.6	19.7	19.8	19.8	19.7	19.9
impulse noise	10.7	10.5	10.5	10.6	10.7	10.6	10.8
jpeg	7.0	6.9	6.9	6.9	6.9	6.8	6.9
motion blur	19.3	17.3	17.1	17.4	17.5	17.6	17.7
pixelate	9.0	8.6	8.5	8.6	8.5	8.5	8.5
saturate	5.9	5.9	5.8	5.8	5.8	5.8	5.9
shot noise	8.8	8.7	8.6	8.7	8.7	8.6	8.7
snow	13.9	13.2	13.1	13.2	13.2	13.2	13.3
spatter	6.5	6.4	6.4	6.4	6.4	6.4	6.4
speckle noise	8.6	8.5	8.4	8.5	8.5	8.5	8.5
zoom blur	54.1	42.3	35.4	34.5	34.3	34.9	35.3
AVERAGE	15.7	14.3	13.8	13.8	13.8	13.8	13.9

Table 13: Performance variation (on IAM) for different number of progressive updates. For Number of Iterations = K , the algorithm is run for K iterations, with $\frac{100}{K}k\%$ of top lines included in the self-training algorithm for iteration number $k \in [1, K]$.

	Number of Iterations						
	1	2	4	6	8	10	12
original	8.4	8.4	8.4	8.4	8.3	8.4	8.4
brightness	11.6	10.9	10.8	10.8	10.7	10.8	10.8
contrast	22.4	13.0	12.4	12.3	12.2	12.2	12.2
defocus blur	39.3	35.0	34.1	34.0	33.9	34.0	34.0
elastic	61.2	62.5	60.5	60.3	60.4	60.2	60.2
fog	11.8	11.2	11.3	11.3	11.2	11.3	11.3
frost	44.4	39.6	39.2	38.9	38.9	39.0	39.0
gaussian blur	30.5	23.7	23.5	23.7	23.2	23.5	23.5
gaussian noise	14.8	14.5	14.8	14.8	14.6	14.7	14.7
glass blur	43.8	32.7	29.4	29.3	29.1	29.2	29.2
impulse noise	28.8	26.0	25.6	25.6	25.7	25.7	25.7
jpeg	14.0	13.1	13.1	13.1	13.0	13.0	13.0
motion blur	35.9	31.0	30.8	30.9	30.8	30.9	30.9
pixelate	15.4	13.5	13.2	13.2	13.1	13.0	13.0
saturate	19.0	13.7	13.4	13.6	13.3	13.4	13.4
shot noise	25.4	24.6	24.7	24.6	24.6	24.6	24.6
snow	59.3	55.4	53.3	53.0	52.9	52.9	52.9
spatter	11.4	11.2	11.4	11.3	11.2	11.3	11.3
speckle noise	25.7	25.0	25.1	25.1	25.1	25.1	25.1
zoom blur	61.1	57.8	52.8	51.5	51.6	51.4	51.4
AVERAGE	29.2	26.1	25.4	25.3	25.2	25.2	25.2

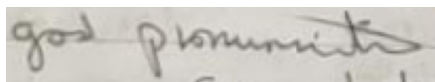
Table 14: Performance variation (on CVL) for different number of progressive updates. For Number of Iterations = K , the algorithm is run for K iterations, with $\frac{100}{K}k\%$ of top lines included in the self-training algorithm for iteration number $k \in [1, K]$.

	Number of Iterations						
	1	2	4	6	8	10	12
original	19.3	17.3	16.8	16.1	16.3	16.4	16.6
brightness	23.5	21.5	19.9	19.7	19.8	19.9	20.2
contrast	24.3	21.9	20.1	19.8	19.8	20.0	20.3
defocus blur	37.5	35.6	33.4	32.6	32.6	32.6	32.9
elastic	25.9	23.9	22.3	22.1	22.2	22.4	22.6
fog	28.4	25.8	24.0	23.7	23.7	24.0	24.0
frost	56.5	54.6	54.8	54.0	54.1	53.9	53.8
gaussian blur	23.6	21.6	19.9	19.6	19.7	19.8	20.1
gaussian noise	23.3	21.2	19.7	19.5	19.6	19.7	19.9
glass blur	27.5	24.7	22.7	22.5	22.5	22.8	23.0
impulse noise	31.1	29.1	27.6	27.5	27.6	27.6	27.8
jpeg	24.6	22.2	20.3	20.1	20.2	20.3	20.5
motion blur	34.7	33.0	31.3	30.8	30.8	31.0	31.1
pixelate	22.8	20.4	18.7	18.7	18.8	18.8	19.1
saturate	21.0	18.9	17.4	17.3	17.5	17.5	17.8
shot noise	26.7	24.7	23.1	23.0	23.1	23.2	23.4
snow	41.7	39.4	38.5	38.6	38.7	39.0	39.0
spatter	21.2	19.2	17.7	17.6	17.8	17.9	18.1
speckle noise	28.7	26.8	25.3	24.9	25.2	25.3	25.4
zoom blur	26.3	24.0	22.1	21.7	21.8	21.8	22.1
AVERAGE	28.4	26.3	24.8	24.5	24.6	24.7	24.9

Table 15: Performance variation (on KOHTD) for different number of progressive updates. For Number of Iterations = K , the algorithm is run for K iterations, with $\frac{100}{K}k\%$ of top lines included in the self-training algorithm for iteration number $k \in [1, K]$.

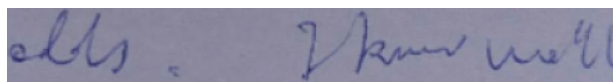
Iter 1: god pronummits
Iter 2: god pronunnite
Iter 3: god pronuncite
Iter 4: god pronunciite

GT: good pronunciation



Iter 1: alls. Ik well
Iter 2: alls. I knew well
Iter 3: adds. I knew we'll
Iter 4: adds. I knew we'll

GT: odds. I know we'll



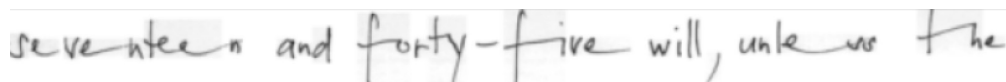
Iter 1: of Viquin-mel talay is closed seorious
Iter 2: of Virginia-mel today is closed reorious
Iter 3: of Virginia-met today is closed ressiions
Iter 4: of Virginia-met today is closed sessions

GT: of Virginia-met today in closed session



Iter 1: seventeen and forty-five will, unle wo the
Iter 2: seventeen and forty-five will, unle wo the
Iter 3: seventeen and forty-five will, unless the
Iter 4: seventeen and forty-five will, unless the

GT: seventeen and forty-five will, unless the



Iter 1: Bahiral
Iter 2: rahiral
Iter 3: ratural,
Iter 4: ratural,

GT: natural



Iter 1: pointment; the other subsequent : the pende
Iter 2: pointment; the other subsequent : the pende
Iter 3: pointment; the other subsequent: the perse
Iter 4: pointment; the other subsequent: the person

GT: -pointment; the other subsequent: the person

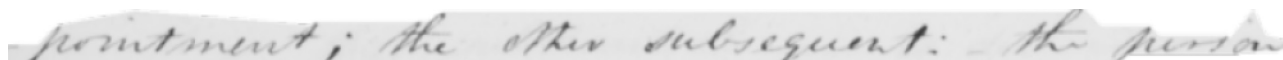


Figure 8: Exemplars showing the predictions over self-training iterations on two images each from the three datasets.

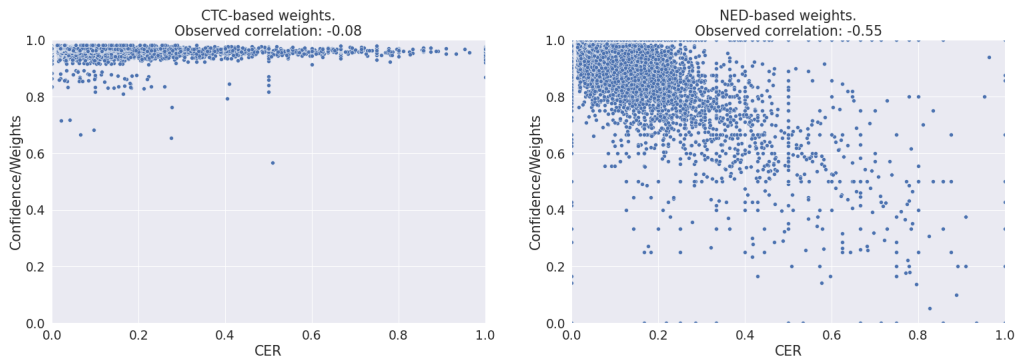


Figure 9: **Correlation between correctness and confidence metric used on ICDAR2015-HTR** Plot of ground-truth CER vs the confidence obtained based on the CTC loss (left), and the confidence obtained using our augmentation based confidence metric (right). Our confidence metric assigns higher values to the lines with lower CER. Whereas, for the same CTC loss based confidence, we observe a wide range of CER, indicating a low correlation with correctness.

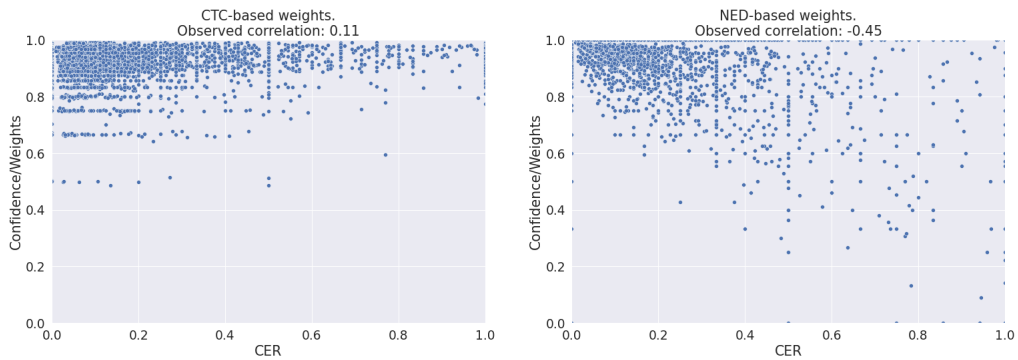


Figure 10: **Correlation between correctness and confidence metric used on GNHK** Plot of ground-truth CER vs the confidence obtained based on the CTC loss (left), and the confidence obtained using our augmentation based confidence metric (right). Our confidence metric assigns higher values to the lines with lower CER. Whereas, for the same CTC loss based confidence, high weights are assigned to the lines irrespective of their CERs, indicating a low correlation with correctness. There is even a positive correlation between the confidence using CTC loss and the CER, which should have been otherwise negative, as more confidence should be assigned to lines with lower CER, i.e., ones which are supposedly less wrong.

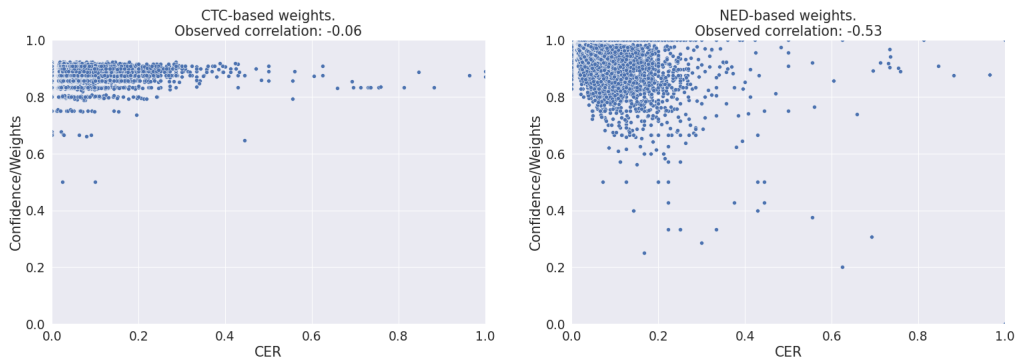


Figure 11: **Correlation between correctness and confidence metric used on IAM** Plot of ground-truth CER vs the confidence obtained based on the CTC loss (left), and the confidence obtained using our augmentation based confidence metric (right). Our confidence metric assigns higher values to the lines with lower CER. Whereas, for the same CTC loss based confidence, high weights are assigned to the lines irrespective of their CERs, indicating a low correlation with correctness.

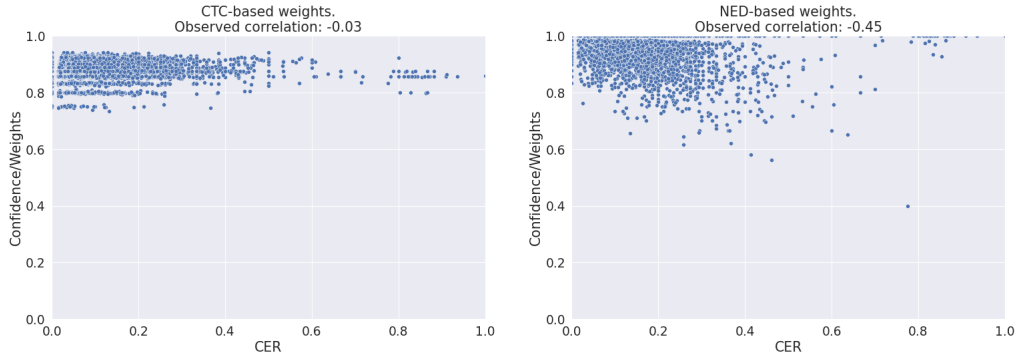


Figure 12: **Correlation between correctness and confidence metric used on CVL** Plot of ground-truth CER vs the confidence obtained based on the CTC loss (left), and the confidence obtained using our augmentation based confidence metric (right). The CTC based metric assigns high confidence values to even those lines with high CER. Our CER based metric is more closely correlated with the error, as observed.

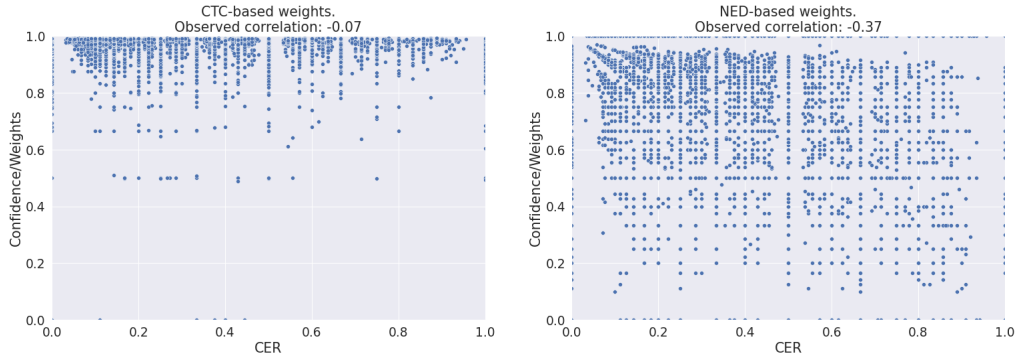


Figure 13: **Correlation between correctness and confidence metric used on KOHTD** Plot of ground-truth CER vs the confidence obtained based on the CTC loss (left), and the confidence obtained using our augmentation based confidence metric (right). The CTC based metric assigns high confidence to lines irrespective of their CERs. The unnatural blockyness of the plot is because the evaluation on this dataset is at a word level, and hence there is an inherent quantization of possible CER.

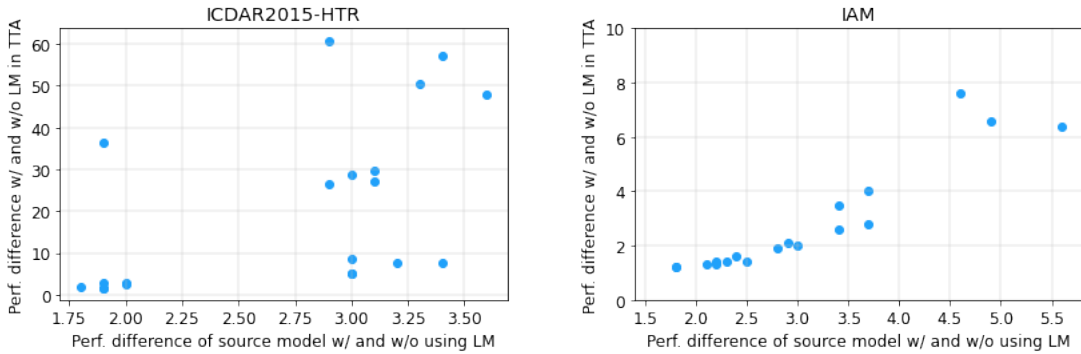
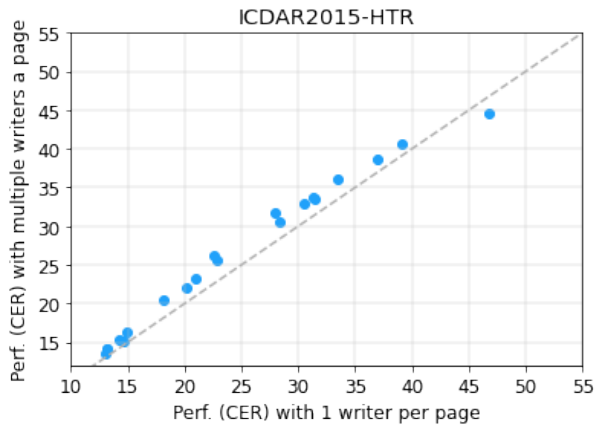
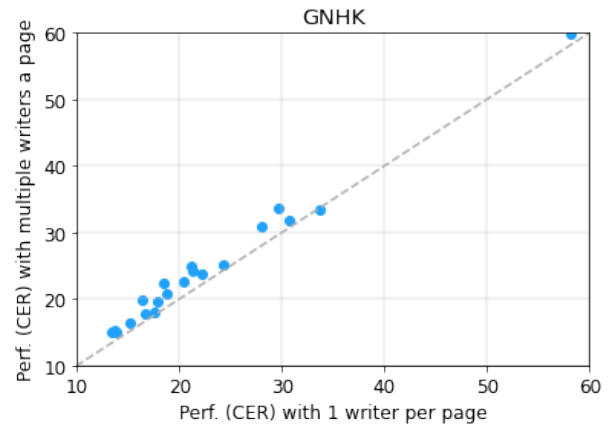


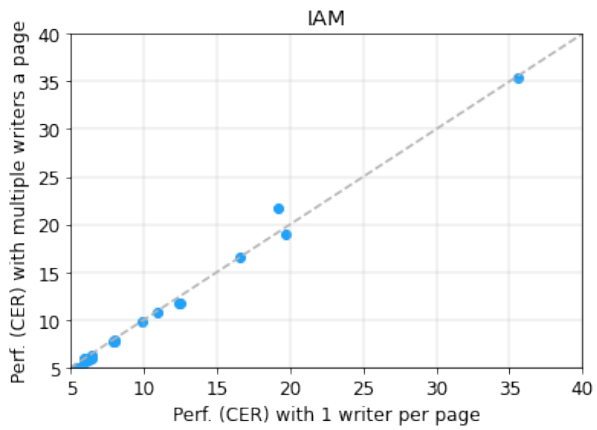
Figure 14: **The role of LM in adapting the optical model for ICDAR2015-HTR and IAM respectively.** Each point here denotes the relative improvement the LM introduces for various corrupted versions of the dataset. The x value of each point is the CER improvement when decoding is done using the LM Decoder vs GreedyDecoder when evaluating the source model. The y-axis shows the CER improvement when our proposed method is used with the LM Decoder vs GreedyDecoder.



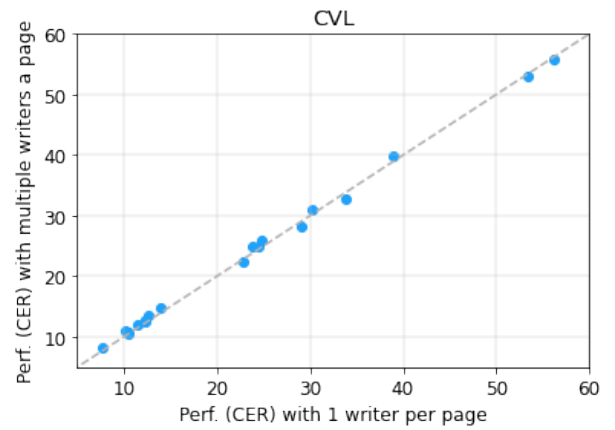
(a) ICDAR2015-HTR



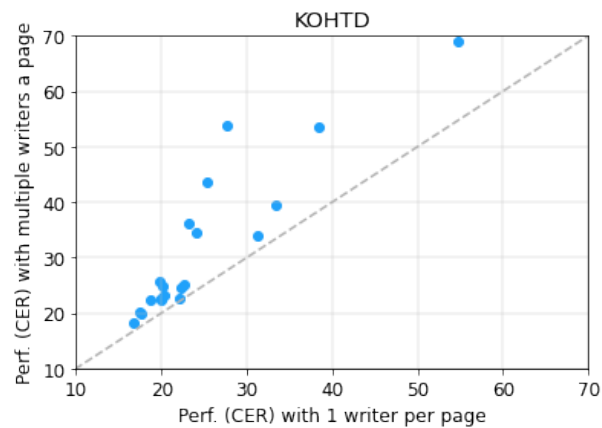
(b) GNHK



(c) IAM



(d) CVL



(e) KOHTD

Figure 15: **Multiple writers in a single page.** Each point denotes results for each corrupted version of the particular dataset in the captions. The x-axis of each point is the performance on the vanilla dataset consisting of one writer per page, and the y-axis of that point shows the performance on the concocted version of the dataset consisting multiple writers in a page.